

# Development of Composite Bipolar Plates for PEMFC

## 1. Introduction

Polymer electrolyte membrane fuel cell (PEMFC) is a very promising power source for residential and mobile applications with its favorable features such as high power density, relatively low operating temperature, convenient fuel supply, long lifetime, etc [1,2]. In spite of those advantages, commercialization of PEMFC is being delayed mainly due to the high fabrication cost. Among the PEMFC components, bipolar plates, for which graphite with machined flow channels are most commonly used, account for as much as 60 % of the stack cost [3]. Hence, for wide-spread commercialization of PEMFC, cost reduction of the bipolar plate is inevitable.

One approach to the cost reduction of PEMFC bipolar plate is to develop new materials with low manufacturing cost such as carbon composites and metal alloys. Cost models estimated that, if using composites or metal alloys, cost of bipolar plates would be only 15 ~ 29 % of the stack costs [4]. In addition to low manufacturing cost, PEMFC bipolar plates require high surface and bulk electronic conductivity, sufficient mechanical strength, chemical stability in the PEMFC environment, gas tightness, and light weight [5]. As a candidate to fulfill those requirements for PEMFC bipolar plate, carbon composite has been developed extensively [5-12]. However, most of the studies investigated material properties of carbon composites or reported that, assembled into a single cell, composite bipolar plates exhibited performance comparable to that of metallic bipolar plates [5-12].

In this study, two kinds of carbon composite were developed and evaluated in terms of the required properties as described above. Single cells were assembled with the composite bipolar plates and their initial and long-term performance was examined in comparison with a single cell employing graphite bipolar plates.

## 2. Experimental

### 2.1. Material tests

Two kinds of carbon composite plate were developed using same compound powder; composite A was manufactured into a plate by hot-pressing the compound powder and then gas channels were machined on its surface to make a bipolar plate; composite B was fabricated directly into a bipolar plate by molding the compound powder with applying compression pressure at an adequate temperature. Thickness of the composite A and B bipolar plates was 2 mm. The compound powder was composed of ~90 % graphite powder, ~10 % unsaturated polymer, and small amount of organic solvent and additives.

Before single cell tests, electrical and physical properties of the carbon composites were

evaluated. Bulk electronic conductivity was measured by the well-known four-point probe technique. A constant current was applied through the two outermost probes, and the resulting voltage across the two innermost probes was measured. To measure contact resistance, an experimental apparatus was devised as depicted in Fig. 1. A specimen with thickness of 2 mm was placed between two carbon papers, each of which was in contact with a copper plate on the opposite side. While a constant current was passed through the two copper plates, potential difference between the copper plates was measured. The measurement was repeated at various compaction pressures applied through the apparatus, in order to examine effects of compaction pressure on the contact resistance. Contact resistance was calculated based on the Ohm's law. For measuring gas tightness, 5 bar of air was applied to one side of a specimen while the other side was vacuumed and gas flow was measured at the vacuum side. To investigate surface energy of a specimen, water contact angle was measured using PCHM 575-4 (Frist Angstrom Co.). Flexural strength, density, and water adsorption were measured following ASTM D 790, 1895, 570, respectively.

## 2.2. Single cell tests

The catalyst ink for the electrodes was prepared by mixing the catalyst powders (40 wt.% Pt/C, E-TEK), Nafion solution, and *iso*-propyl alcohol. Then the prepared catalyst ink was sprayed on the wet-proofed carbon paper with platinum loading of 0.4 and 0.7 mg/cm<sup>2</sup> for anode and cathode, respectively. Membrane-electrode assembly (MEA) was fabricated by placing the electrodes at both sides of the pre-treated Nafion 115 membrane, followed by hot pressing at 140 °C and 200 kg/cm<sup>2</sup> for 90 s. The active electrode area was 25 cm<sup>2</sup>.

Single cell was constructed from the prepared MEA, Teflon gasket, and the prepared graphite and composite bipolar plates on both sides of the MEA. Thickness of the bipolar plates was 2 mm. Hydrogen and oxygen gases were fed to the anode and cathode, respectively, after passing through a bubble humidifier, and stoichiometry of the fuel and the oxidant was 1.5 and 3, respectively. Operating temperature and pressure were 80 °C and 1 atm, respectively. Performance of the single cell was evaluated by measuring the *I-V* characteristics using an electronic loader (Daegil Electronics, EL 500P). Polarization resistance of the single cells was investigated by measuring AC impedance of the single cells with the oxygen electrode as the working electrode and the hydrogen electrode as the reference and counter electrode. The counter electrode also served as a reference electrode, since the overpotential at the counter electrode for the hydrogen oxidation or evolution reaction is negligible [13]. IM6 (ZAHNER) was used for the impedance measurement and the applied frequency was varied from 1 mHz to 10 kHz with an excitation voltage of 5 mV (peak-to-peak).

### 3. Results and Discussion

#### 3.1. Electrical and Physical Properties

Low electrical bulk and contact resistance are essential features for PEMFC bipolar plates. Using the four-point probe technique, bulk resistivity of graphite, composite A, and composite B was measured to be 16.85, 131.1, and 151.6  $\Omega$  cm, respectively. Bulk resistivity of the carbon composites was 8 ~ 9 times higher than that of graphite. However, it was just slightly higher than the target value of 100  $\Omega$  cm [6]. In operating a fuel cell, contact resistance would have a stronger effect on cell performance than bulk resistivity since the contact resistance includes bulk resistance of bipolar plate and carbon diffusion layer as well as interfacial resistance between bipolar plates and carbon diffusion layers. Contact resistance of graphite, composite A, and composite B was measured at various compaction pressures using the experimental apparatus shown in Fig. 1 and the results are presented in Fig. 2. With increasing compaction pressure, contact resistance of the materials decreased rapidly at low compaction pressures and then decreased gradually at high compaction pressures. At a given compaction pressure, contact resistance increased in the order of graphite < composite A < composite B; at a compaction pressure of 180 N cm<sup>-2</sup>, contact resistance of graphite, composite A, and composite B were measured to be 30.2, 31.7, 33.4 m $\Omega$  cm<sup>2</sup>, respectively. The result shows that, even though bulk resistivity of the carbon composites was higher than that of graphite, contact resistance of the carbon composites is almost same as that of graphite. This could be attributed to the fact that by compressing the carbon composite, carbon powders formed a compact network. Thus, ohmic resistance of a single cell is expected to be similar for the graphite and the carbon composite bipolar plates.

In addition to low electrical resistance, bipolar plate materials require sufficient mechanical strength, chemical stability in the PEMFC environment, gas tightness, light weight, and low water absorption. Table 1 summarizes those properties of graphite, composite A, and composite B. Except flexural strength, all the requirements were fairly satisfied except flexural strength; flexural strength of composite A and B were 394 and 209 kg<sub>f</sub> cm<sup>-2</sup> and the target was 500 kg<sub>f</sub> cm<sup>-2</sup>. At present, low flexural strength seems to be the primary disadvantage of the carbon composites developed in this study. However, in manufacturing and operating single cells, any of the composite bipolar plates was not broken under the normal cell assembling and operating condition. Relatively high flexural strength of composite A shows prospects of the carbon composites. Composite A and B were made from the same compound powder and processed differently. Therefore, it seems that there is a margin for improvement of flexural strength of composite B by optimizing the molding condition.

It was found that wettability was one of the important features affecting on cell performance particularly at high current densities [15,16]. The lower the surface energy of

bipolar plates was, the more readily flooding occurred at the cathode side. As a measure of surface energy, water contact angle of graphite, composite A, and composite B was measured and presented in Fig. 3. Water contact angle of composite A was slightly lower than that of graphite and composite B, reflecting a lower surface energy of composite A. Thus, it can be predicted that composite A bipolar plates would be more likely to flood than graphite and composite B bipolar plates.

### 3.2. Cell performance

Fig. 4 presents initial performance of the single cells assembled with graphite, composite A, and composite B bipolar plates. Open circuit voltage (OCV) of the single cells was almost same to be 1.0 V. At low current densities, the single cells exhibited almost same performance. At intermediate current densities, composite bipolar plates showed slightly lower performance than graphite bipolar plates; at a cell voltage of 0.6 V, current density of the single cells using graphite, composite A, and composite B bipolar plates was 996, 948, and 992 mA cm<sup>-2</sup>, respectively. With increasing current density higher than 1 A cm<sup>-2</sup>, voltage of the single cell using composite A bipolar plates decreased more rapidly than that of the single cells using graphite and composite B bipolar plates, resulting from the lower surface energy of composite A, as shown in Fig. 3. Composite A bipolar plate with a low surface energy could retain more water produced by the cathode reaction and supplied through a humidifier, resulting in the mass transfer polarization.

To examine ohmic and charge transfer resistance of the single cells, electrochemical impedance spectroscopy was carried out at 0.85 V and Nyquist plots were plotted as shown in Fig. 5. The applied cell voltage was IR-corrected. The Nyquist plots are semi-circular; the left point of intersection with the *x*-axis corresponds to the ohmic resistance and the diameter of the semi-circle to the charge transfer resistance [17]. In the AC impedance measurement, oxygen electrode served as the working electrode and hydrogen electrode as the counter electrode. The counter electrode also served as the reference with its negligible overpotential for the hydrogen oxidation or evolution reaction [13]. Thus, the charge transfer resistance obtained through the AC impedance study primarily could be attributed to the oxygen reduction reaction. From the data in Fig. 5, for the single cells using graphite, composite A, and composite B bipolar plates, ohmic resistance was calculated to be 8.95, 7.42, and 7.14 mΩ cm<sup>2</sup>, respectively, and charge transfer resistance to be 40.1, 38.1, and 38.2 mΩ cm<sup>2</sup>, respectively. Ohmic and charge transfer resistance of the single cells using composite bipolar plates were almost same and slightly lower than those using graphite bipolar plates. Thus, if the properties of MEAs and cell assemblies of the single cell using graphite bipolar plates were identical to those of the single cells using composite bipolar plates, the cell performance would exhibit slightly better than presented in

Fig. 4. However, the differences in the properties of the MEAs and cell assemblies revealed in Fig. 5 are in the range of error.

Fig. 6 compares initial and long-term performance of the single cells assembled with graphite, composite A, and composite B bipolar plates, demonstrating that degradation of the single cells was negligible except in mass transfer region. In the initial operation, graphite and composite B bipolar plates did not exhibit mass transfer polarization, which was observed in the long-term operation. Mass transfer polarization in the long-term operation could be associated with the residual water produced and supplied during the operations. Those results reflect that composite A bipolar plates with a relatively low surface energy retained water even in the very initial operation while graphite and composite B bipolar plates with a high surface energy retained water as operation proceeded for enough water to be produced. Current density at a cell voltage of 0.6 V was plotted as a function of operation time in Fig. 7. During the 500-hr operation, performance of all the bipolar plates was maintained without degradation. All those results presented in Figs 4 through 7 demonstrate that the carbon composite bipolar plates developed in this study have comparable initial and long-term performance to graphite bipolar plates and can be alternative bipolar plate materials to substitute the high-cost machined graphite.

#### 4. Conclusions

Two kinds of carbon composite were developed and tested as a candidate for PEMFC bipolar plates in comparison with machined graphite. Both of the carbon composite fairly satisfied the development targets of PEMFC bipolar plates, with regard to electrical and physical properties. In initial and long-term operation, performance of the composite bipolar plates was comparable to that of graphite bipolar plates. In spite of similar bulk and contact resistance of the carbon composites, composite B bipolar plates showed slightly better performance than composite A bipolar plates, particularly at high current densities, due to the higher surface energy resulting in the better water removal. All those results show that carbon composite A and B are very promising candidates for PEMFC bipolar plates.

#### References

1. S. Srinivasan, *J. Electrochem. Soc.*, **136** (1989) 41C.
2. S. J. Lee and S. Mukerjee, *Electrochim. Acta*, **43** (1998) 3693.
3. D. P. Davies, P. L. Adcock, M. Turpin, and S. J. Rowen, *J. Applied Electrochemistry*, **30** (2000) 101.
4. I. B.-O, R. Kirchain, and R. Roth, *J. Power Sources*, **109** (2002) 71.
5. T. M. Besmann, J. W. Klett, J. J. Henry, Jr., and E. L.-Curzio, *J. Electrochem. Soc.*, **147**

- (2000) 4083
6. D. N. Busick and M. S. Wilson, *Fuel Cell Bulletin*, **2** (1999) 6
  7. J. Scholta, B. Rohland, V. Trapp, and U. Focken, *J. Power Sources*, **84** (1999) 231.
  8. H. Maeda, A. Yoshimura, H. Fukumoto, and T. Hayashi, *Abstracts of Fuel Cell Seminar* (2002) 58.
  9. A. Heinzl, H. Kraus, C. Kreuz, F. Mahlendorf, and O. Niemzig, *Abstracts of Fuel Cell Seminar* (2002) 153.
  10. Stewart Jr. and C. Robert, US patent 4,670,300, 2 June (1987)
  11. T. Uemura and S. Murakami, US patent 4,737,421, 12 April (1988)
  12. D. Busick and M. Wilson, US patent 6,248,467, 19 June (2001)
  13. X. Cheng, B. Yi, M. Han, J. Zhang, Y. Qiao, and J. Yu, *Journal of Power Sources*, **79** (1999) 75.
  14. V. Mehta, J. S. Cooper, *J. Power Sources* **114** (2003) 32.
  15. U.-S. Jeon, E. A. Cho, H. Y. Ha, S.-A. Hong, and I.-H. Oh, "Development of Metallic Bipolar Plates for Polymer Electrolyte Membrane Fuel Cells Based on 316 Stainless Steel", in preparation for publication in the *Journal of Power Sources* (2003).
  16. A. J. Cisar, O. J. Murphy, K-T. Jeng, C. Salinas, S. Simpson, D. Weng, US Patent 6,426,161, 30 Jul. (2002)
  17. A. J. Bard, *Electrochemical Methods*, John Wiley & Sons, p. 351 (1980)

Table 1. Electrical and physical properties of graphite and carbon composite plates [6,8,14].

	Graphite	Composite A	Composite B	Target	Reference
Bulk resistivity ( $\Omega$ cm)	16.85	131.1	151.6	< 100	ASTM C611
Flexural strength ( $\text{kg}_f \text{cm}^{-2}$ )	674	394	209	> 500	ASTM D790
Density ( $\text{g}/\text{cm}^3$ )	1.95	1.69	1.82	< 5	ASTM D1895
Gas tightness (at 5 bar)	No leak	No leak	No leak	No leak at 5 bar	-
Water absorption (%)	0	0.133	0.287	< 0.3	ASTM D570
Depth deviation of flow channels ( $\mu\text{m}$ )	0.2597	0.265	2.556	< 3.0	Alpha step

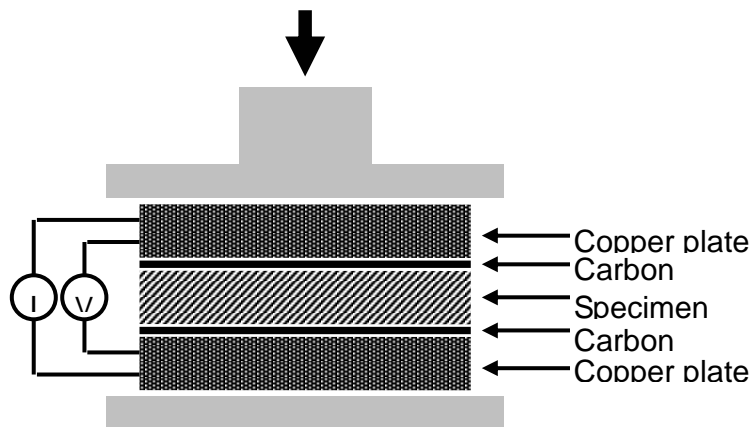


Fig. 1. A schematic diagram of the experimental apparatus used for contact resistance measurement.

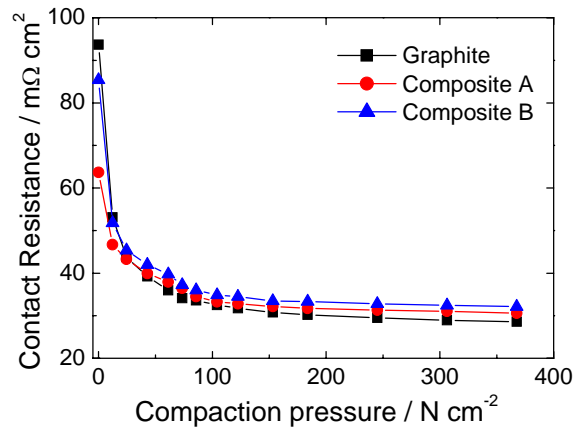


Fig. 2. Contact resistance of graphite, composite A, and composite B measured at various compaction pressures.

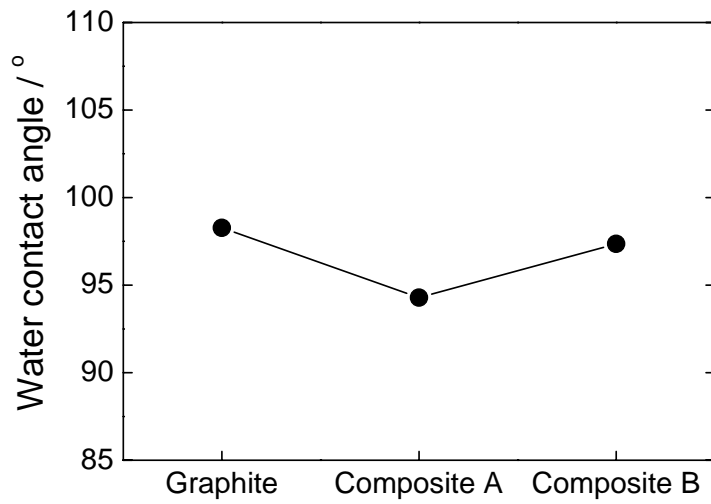


Fig. 3. Water contact angle of graphite, composite A, and composite B.



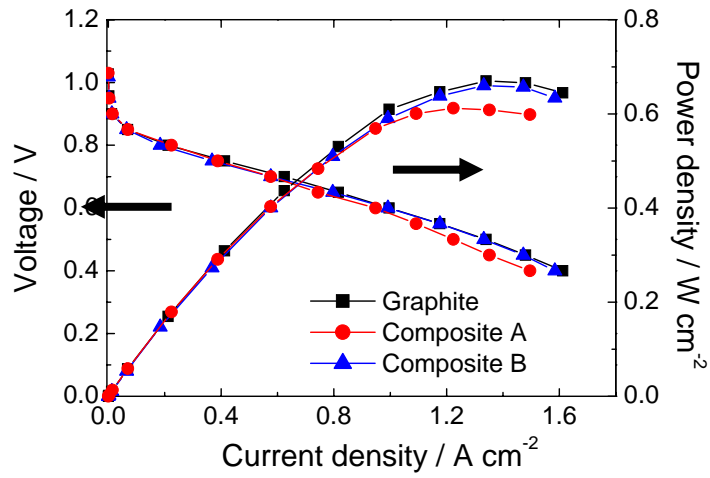


Fig. 4. Initial performance of the single cells assembled with graphite, composite A, and composite B bipolar plates; operating temperature = 80 °C; operating pressure = 1 atm;  $\lambda_{\text{H}_2} = 1.5$  and  $\lambda_{\text{O}_2} = 3$ .

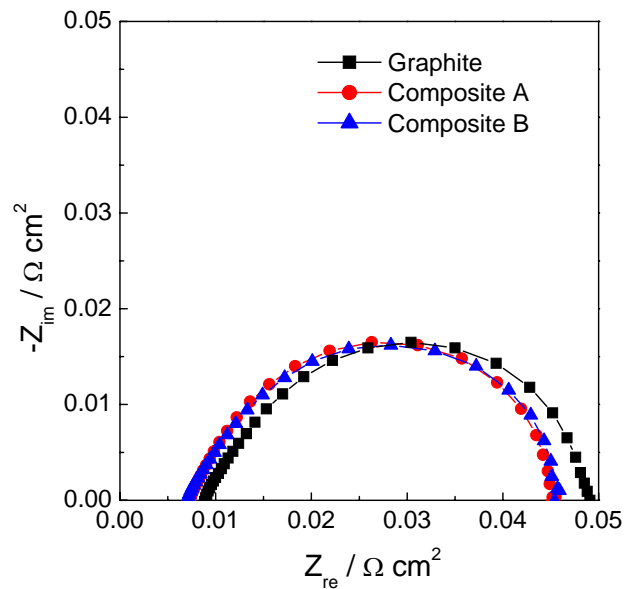


Fig. 5. Initial Nyquist plots for the single cells assembled with graphite, composite A, and composite B bipolar plates; cell temperature = 80 °C; cell voltage = 0.85 V.

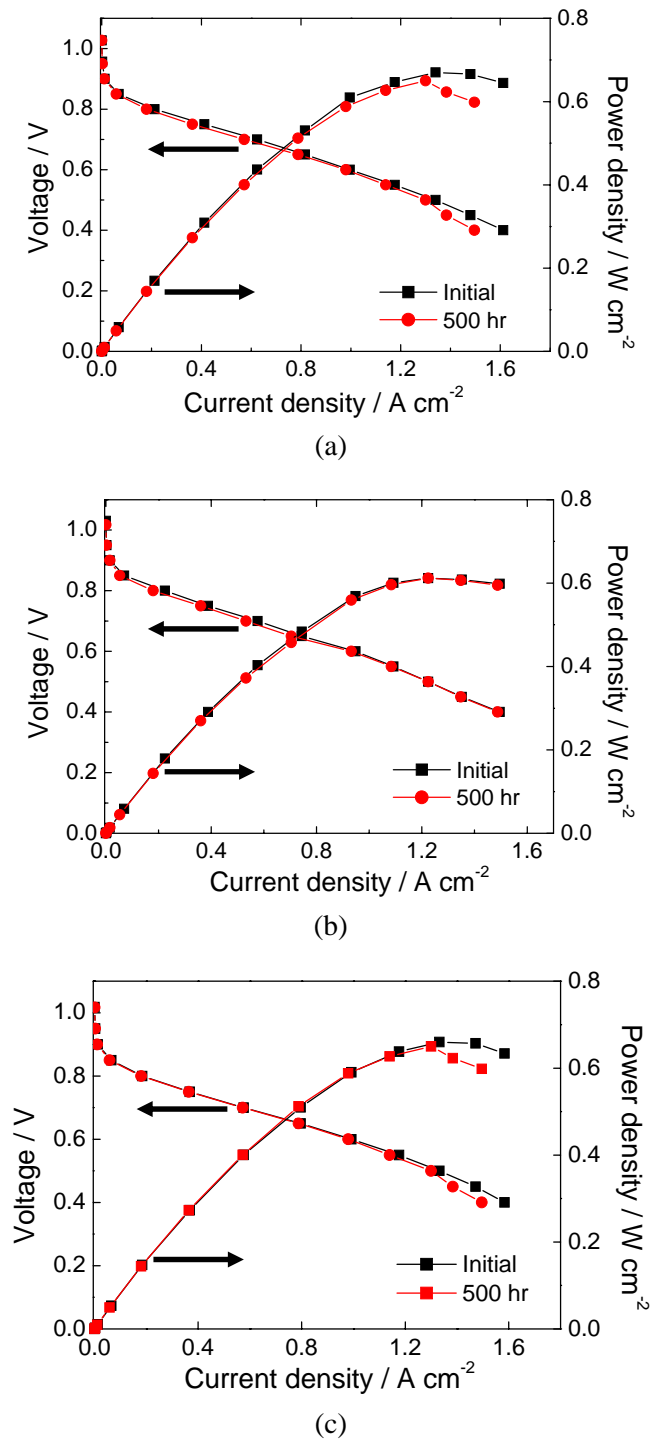


Fig. 6. Effects of 500-hr operation on performance of the single cells assembled with (a) graphite, (b) composite A, and (c) composite B bipolar plates; operating temperature = 80 °C; operating pressure = 1 atm;  $\lambda_{\text{H}_2} = 1.5$  and  $\lambda_{\text{O}_2} = 3$ .

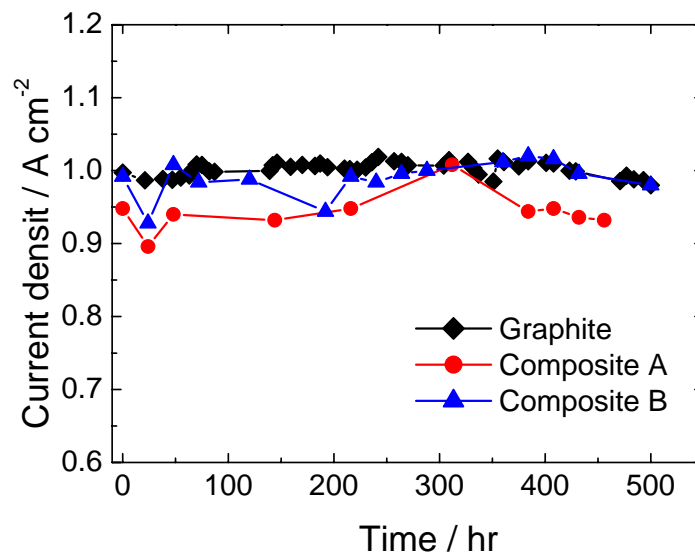


Fig. 7. Long-term performance of the single cells assembled with graphite, composite A, and composite B bipolar plates measured at a cell voltage of 0.6 V; operating temperature = 80 °C; operating pressure = 1 atm;  $\lambda_{H_2} = 1.5$  and  $\lambda_{O_2} = 3$ .